THE JOURNAL OF PHYSICAL CHEMISTRY C

Article

pubs.acs.org/JPCC

Tunable Donnan Potential and Electrokinetic Flow in a Biomimetic Gated Nanochannel with pH-Regulated Polyelectrolyte Brushes

Zachary Milne,[†,§] Li-Hsien Yeh,*[,‡,§] Tzung-Han Chou,[‡] and Shizhi Qian*[,†]

[†]Institute of Micro/Nanotechnology, Old Dominion University, Norfolk, Virginia 23529, United States

[‡]Department of Chemical and Materials Engineering, National Yunlin University of Science and Technology, Yunlin 64002, Taiwan

ABSTRACT: Learning from nature, many experimental results have revealed that biomimetic nanofluidics functionalized by pH-regulated polyelectrolyte (PE) brushes have significant potential for next-generation biosensing devices. The present study theoretically investigates for the first time the field effect on the Donnan potential and electrokinetic flow (EKF) in a biomimetic PE-modified nanochannel. The results obtained show that, in addition to the thickness and softness of the PE brush layer, the EKF velocity is tunable by modulating the Donnan potential of PE-modified nanochannels with a nanofluidic field effect transistor under various solution properties including pH and background salt concentration. The electrostatic gating effect on the Donnan potential depends significantly on the solution properties, but insignificantly on the thickness of the PE brush layer.

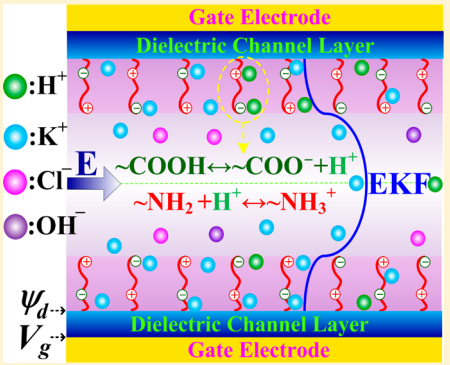

1. INTRODUCTION

Recent progress in nanofabrication allows for the use of nanofluidics, such as nanopores and nanochannels, for versatile applications, including energy conversion,[1,2] nanofluidic diodes,[3−8] single (bio)nanoparticle sensing,[9−11] and separation of biomolecules.[12,13] Many experimental results demonstrate that the feasibility of these applications relies on actively manipulating the charge properties of these nanofluidic devices in contact with aqueous solution. To achieve charge manipulation, a nanofluidic field effect transistor (FET),[14−19] referring to an electrically controllable gate electrode embedded within the dielectric nanochannel (or nanopore) trench, has been developed. The charge property and, accordingly, the electrokinetic transport of fluid, ions, and (bio)nanoparticles in gated nanofluidic devices can be tuned by modulating the potential applied to the gate electrode. Therefore, a comprehensive understanding of how the FET-gated nanofluidics functions in various solution mediums is essential for the advance in next-generation nanofluidics-based devices.

Numerous theoretical studies on the electrokinetic transport of fluid, ions, and (bio)nanoparticles in the gated nanofluidic devices have been conducted.[20−30] Adopting the Poisson−Nernst−Planck (PNP) model coupled with the Navier−Stokes (NS) equations, Daiguji et al.,[20,21] for example, investigated the ion transport[20] and the ion current rectification (ICR)[21] phenomena in a gated nanochannel. They concluded that the electrostatic gating effect on the ion transport and ICR behaviors was substantial. Singh and Kumar[22] research into the effects of the gate electrode's length and the dielectric layer's thickness on the ion and fluid transport in a gated nanochannel, and revealed that the FET control of the ionic current was enhanced with an increase in the gate electrode's length and a decrease in the thickness of dielectric layer. A similar model was adopted by Jin and Aluru,[23] and Pardon and van der Wijngaart[24] to analyze the ion transport in an electrically gated nanochannel. FET control was also used by He et al.[25] to enhance the DNA capture rate into a nanopore, and by Ai et al.[26] and He et al.[27] to control DNA translocation through a nanopore in the nanopore-based DNA sequencing technology. Recently, Yeh et al.,[28] Hughes et al.,[29] and Xue et al.[30] derived a series of analytical solutions for the surface charge property, the electroosmotic flow, as well as the streaming conductance in a FET-gated nanochannel. They found that the performance of the FET depended significantly on the pH and the concentration of the electrolyte solution.

However, previous theoretical analyses on the FET control primarily concentrated on solid-state nanofluidic devices.[20−30] Inspired by nature, polyelectrolyte (PE) brush-functionalized nanofluidics, solid nanochannels, or nanopores chemically modified by PE brushes, have recently emerged as innovative tools for regulating ion transport and current[4,31−34] and sensing biomolecules.[35−37] In these PE-modified nanofluidic devices, the Donnan potential at the PE layer/dielectric channel interface,[38,39] instead of the conventional zeta potential adopted in solid-state nanofluidic devices, governs the transport of fluid and ions. Recently, Benson et al.[40] investigated the field control of the Donnan potential and the electrokinetic flow (EKF) in a PE-modified nanochannel and found that the PE layer made the field effect more complicated. In their model, the PE layer carries homogeneous fixed charges, implying that its charge density is independent of pH and concentration of the electrolyte solution.

Received: May 9, 2014
Revised: August 1, 2014
Published: August 5, 2014

dx.doi.org/10.1021/jp504588b | J. Phys. Chem. C 2014, 118, 19806−19813

In living cells, the charge properties of biological ion channels can be modulated by an external stimulus,[6] implying that their charges are strongly dependent on the solution environments like pH and salt concentration due to the deprotonation and protonation reactions of functional groups on biological ion channels. Inspired by this, numerous studies have been conducted by using pH-tunable PE brush-functionalized nanochannels as biomimetic smart nanochannels for versatile applications.[6,7] Considering the growing expansion of relevant applications using these biomimetic nanofluidics, this study investigates, for the first time, the FET control of the Donnan potential and the EKF in a nanochannel with a layer of pH-tunable, zwitterionic, PE brushes, referred to as a PE-modified nanochannel. The key practical parameters including the background salt concentration, pH, and the properties (thickness and softness) of the PE brush layer on the FET control of the Donnan potential and the EKF velocity are investigated.

2. MATHEMATICAL MODEL

Figure 1 depicts the schematic of the PE-modified nanochannel, which comprises a dielectric nanochannel and a layer of

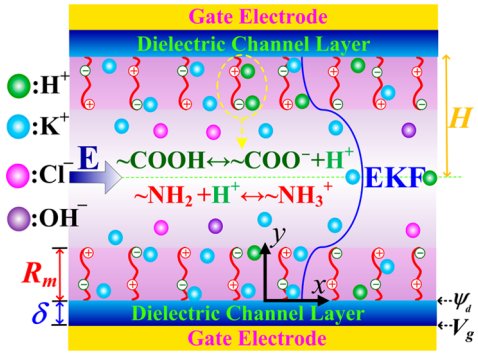

Figure 1. Schematics of the FET control of the Donnan potential (ψ_d) and the electrokinetic flow (EKF) in a pH-tunable, PE-modified nanochannel filled with an electrolyte solution containing four ionic species: H^+, K^+, Cl^-, and OH^-. The blue line depicts the profile of the EKF velocity.

homogeneously structured PE brushes end-grafted to the inner channel wall. The uniform thickness of the PE layer is R_m, and half height of the nanochannel is H. The FET includes a thin dielectric layer of thickness δ and a gate electrode fabricated on the outer surface of the dielectric layer. Cartesian coordinate, (x, y), with the origin located at the bottom solid channel/PE layer interface is used in this study. A uniform electric field **E** of strength E_x is externally applied parallel to the PE-modified nanochannel to generate the EKF, which is controlled by the Donnan potential, ψ_d, through modulating the gate potential, V_g, imposed on the gate electrode. For convenience, we assume that the Donnan potential, ψ_d, considered in this study is the electrical potential at the solid channel/PE layer interface.

The following assumptions are used in this study: (i) The nanochannel is filled with a viscous, Newtonian, incompressible fluid containing N types of ionic species, and the EKF is fully developed along the channel (i.e., x-direction). (ii) The homogeneous PE layer is ion-penetrable and its morphology deformation[41] is not considered in this study. (iii) The properties of the fluid such as viscosity and permittivity within the PE layer are the same as those outside it.[42,43] (iv) The dielectric channel/PE layer interface is uncharged. (v) No-slip plane with zero fluid velocity occurs at the dielectric channel/PE layer interface. (vi) The nanochannel's length and width are much larger than its height; therefore, the considered problem can be viewed as a nanoslit between two parallel plates. (vii) The half height of the nanochannel is much larger than the thickness of the electrical double layer (EDL), $\lambda_D = \kappa^{-1}$. Under this condition, the EDLs of the two parallel plates do not overlap in the y-direction. This assumption is valid for most experimental conditions in nanofluidic applications. For example, the electrolyte concentration in typical nanofluidic experiments ranges from 1 to 1000 mM, yielding the corresponding λ_D varying from 9.6 to 0.3 nm, which is much smaller than the half height in most nanofluidic devices.[12,44,45] Therefore, the effect of ion concentration polarization[46−48] stemming from the selective transport of cations and anions in nanochannels can be ignored. Under the aforementioned assumptions, the electrical potential stemming from the charged PE layers, concentrations of ionic species, and the EKF velocity are uniformly distributed along the x-direction.

Molecular chains in biological systems typically show a pH regulation nature, implying that their charges are highly dependent on the local proton concentration. To mimic this pH tunable nature, the PE brushes are assumed to carry zwitterionic functional groups (e.g., lysine), PE~COOH and PE~NH_2, which have the following dissociation/association reactions:

$$\begin{aligned} &\text{PE}{\sim}\text{COOH} \leftrightarrow \text{PE}{\sim}\text{COO}^- + \text{H}^+, \\ &\text{PE}{\sim}\text{NH}_2 + \text{H}^+ \leftrightarrow \text{PE}{\sim}\text{NH}_3^+ \end{aligned} \tag{1}$$

The equilibrium constants of the above reactions are, respectively, $K_A = N_{\text{PE}\sim\text{COO}^-}[\text{H}^+]/N_{\text{PE}\sim\text{COOH}}$ and $K_B = N_{\text{PE}\sim\text{NH}_3^+}/N_{\text{PE}\sim\text{NH}_2}[\text{H}^+]$, with $[\text{H}^+]$ and N_j being the molar concentration of H^+ ions and the volume site density of the jth functional group (j = PE~COOH, PE~COO^-, PE~NH_2, and PE~NH_3^+). The total site densities of acidic and basic functional groups are $N_A = N_{\text{PE}\sim\text{COO}^-} + N_{\text{PE}\sim\text{COOH}}$ and $N_B = N_{\text{PE}\sim\text{NH}_3^+} + N_{\text{PE}\sim\text{NH}_2}$, respectively. Assuming that the concentration of H^+ ions follows the Boltzmann distribution, $[\text{H}^+] = [\text{H}^+]_0 \exp(-F\psi/RT)$, the volume charge density within the PE layer becomes the following:

$$\begin{aligned} \rho_m &= F(-N_{\text{PE}\sim\text{COO}^-} + N_{\text{PE}\sim\text{NH}_3^+}) \\ &= F\left\{ -\frac{K_A N_A}{K_A + [\text{H}^+]_0 \exp\left(-\frac{F\psi}{RT}\right)} \right. \\ &\quad \left. + \frac{K_B N_B [\text{H}^+]_0 \exp\left(-\frac{F\psi}{RT}\right)}{1 + K_B [\text{H}^+]_0 \exp\left(-\frac{F\psi}{RT}\right)} \right\} \end{aligned} \tag{2}$$

In the above, $[\text{H}^+]_0$ is the bulk molar concentration of H^+ ions; ψ is the electrical potential; R, T, F are, respectively, the universal gas constant, absolute temperature, and Faraday constant.

Suppose that the background electrolyte is KCl and its pH (= $-\log[\text{H}^+]_0$) is adjusted by KOH and HCl. Four major ionic species (i.e., N = 4) including H^+, K^+, Cl^-, and OH^- are considered. Let C_{i0} (in mM), i = 1, 2, 3, and 4, be the bulk concentrations of these ions, respectively, and C_{KCl} be the background salt concentration. Electroneutrality yields the

dx.doi.org/10.1021/jp504588b | J. Phys. Chem. C 2014, 118, 19806−19813

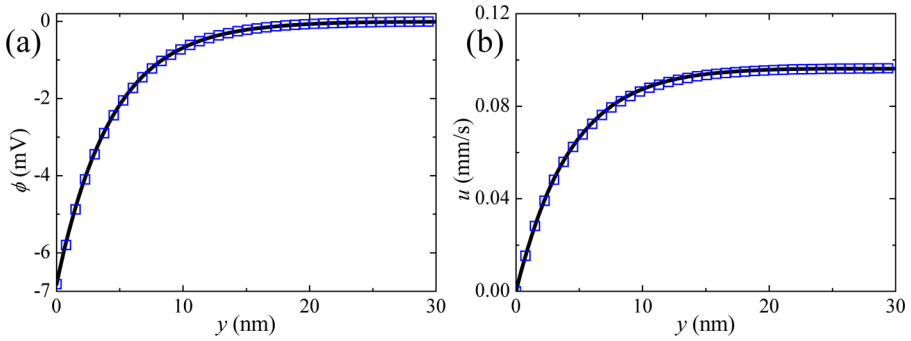

Figure 2. Variations of the electrical potential ϕ (a), and the EKF velocity, u(b) in the y-direction, at E_x = 20 kV/m, pK_A = 2.5, pK_B = 8.5, N_A = 600 mol/m^3, N_B = 600 mol/m^3, pH = 8, C_{KCl} = 5 mM, λ_m = 10^{11} nm, R_m = 0.1 nm, and V_g = 0 V.

following relations for the bulk ionic concentrations:[49,50] $C_{10} = 10^{(-pH+3)}$ and $C_{40} = 10^{-(14-pH)+3}$; $C_{20} = C_{KCl}$ and $C_{30} = C_{KCl}+10^{(-pH+3)}-10^{-(14-pH)+3}$ for pH ≤ 7; and $C_{20} = C_{KCl} - 10^{(-pH+3)} + 10^{-(14-pH)+3}$ and $C_{30} = C_{KCl}$ for pH > 7.

On the basis of the above assumptions, the electrical potentials within the dielectric layer and liquid, ψ and ϕ, respectively, and the EKF velocity, u, are governed by the following:[40]

$$\frac{d^2\psi}{dy^2} = 0, \quad -\delta \le y \le 0 \tag{3}$$

$$\frac{d^2\phi}{dy^2} = -\frac{\rho_e + h\rho_m}{\varepsilon_0\varepsilon_f} = -\frac{1}{\varepsilon_0\varepsilon_f}\sum_{i=1}^{4} Fz_iC_{i0}\exp\left(-\frac{z_iF\phi}{RT}\right) - \frac{h\rho_m}{\varepsilon_0\varepsilon_f}, \quad 0 \le y \le H \tag{4}$$

$$\frac{d^2u}{dy^2} = -\frac{E_x}{\mu}\sum_{i=1}^{4} Fz_iC_{i0}\exp\left(-\frac{z_iF\phi}{RT}\right) + \frac{hu}{\lambda_m^2}, \quad 0 \le y \le H \tag{5}$$

Here, ρ_e is the mobile space charge density; z_i is the valence of the ith ionic species; ε_0 and ε_f are the absolute permittivity of vacuum and the relative permittivity of the liquid phase, respectively; μ is the dynamic fluid viscosity; h is the unit region function (h = 1, the region inside the PE layer; h = 0, the region outside it); $\lambda_m = (\mu/\gamma_m)^{1/2}$ is the softness (or Brinkman screening length) of the PE layer with γ_m being the hydrodynamic frictional coefficient of that layer.

The boundary conditions for eqs 3−5 are as follows:

at the gate electrode ($y = -\delta$),

$$\psi = V_g \tag{6}$$

at the dielectric solid channel/PE layer interface (y = 0),

$$\psi = \phi = \psi_d \tag{7a}$$

$$-\varepsilon_0\varepsilon_d\frac{d\psi}{dy} + \varepsilon_0\varepsilon_f\frac{d\phi}{dy} = 0 \tag{7b}$$

$$u = 0 \tag{7c}$$

at the PE layer/liquid interface ($y = R_m$),

$$\phi|_{y=R_m^-} = \phi|_{y=R_m^+} \tag{8a}$$

$$\left.\frac{d\phi}{dy}\right|_{y=R_m^-} = \left.\frac{d\phi}{dy}\right|_{y=R_m^+} \tag{8b}$$

$$u|_{y=R_m^-} = u|_{y=R_m^+} \tag{8c}$$

$$\left.\frac{du}{dy}\right|_{y=R_m^-} = \left.\frac{du}{dy}\right|_{y=R_m^+} \tag{8d}$$

and at the center of the nanochannel ($y = H$),

$$\phi = \frac{d\phi}{dy} = 0 \tag{9a}$$

$$\frac{du}{dy} = 0 \tag{9b}$$

In the above, ε_d is the relative permittivity of the dielectric layer. Equation 7a denotes that the electrical potential is continuous at the dielectric solid channel/PE layer interface; however, the transverse electric field, as depicted in eq 7b, is not continuous because of the difference in the dielectric permittivities (ε_f and ε_d) at that interface. The "0" term on the right-hand side of eq 7b arises from the assumption that the nanochannel/PE layer interface is uncharged as described previously. Equations 8a−8d depict that the electrical potential, and both electric and flow fields are continuous at the PE layer/liquid interface. Equation 9a expresses that at the center of the nanochannel, the electrical potential arising from the charged PE layer vanishes and the ionic concentrations reach their bulk values (due to the assumption of no EDLs overlapping i.e., H ≫ λ_D).

3. RESULTS AND DISCUSSION

The present problem is numerically solved by COMSOL Multiphysics (version 3.5a), which has been used to numerically simulate the electrokinetic transport in PE-modified nanopores without FET control,[43,47,51−53] and in solid-state nanopores with FET.[18,24−27] For illustration, we consider a biomimetic FET-gated silica nanochannel with a relative permittivity ε_d = 3.9 (SiO_2),[26] a thickness of dielectric layer δ = 30 nm, and the half height H = 100 nm under an application of uniform electric field E_x = 20 kV/m. To simulate pH-tunable and zwitterionic characteristics of biomimetic nanochannels, we consider the constitution of the PE layer consisting of amino acid-like PE chains with lysine groups[4,31] with pK_A = 2.5 (α-carboxyl), pK_B = −8.5 (α-amino),[54] and N_A = N_B = 600 mol/m^3.[55] Consequently, the isoelectric point (IEP) of the PE layer is 5.6. The softness degree of the soft layer, λ_m, is set to 1 nm,

dx.doi.org/10.1021/jp504588b | J. Phys. Chem. C 2014, 118, 19806−19813

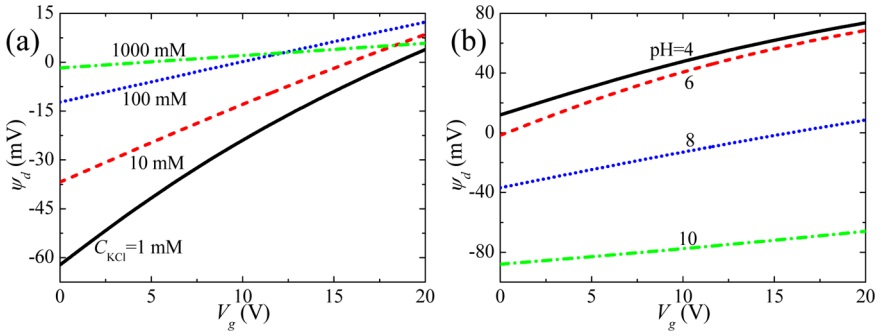

Figure 3. Variations of the Donnan potential ψ_d with the gate potential V_g for various C_{KCl} at pH = 8, (a), and for various solution pH at C_{KCl} = 10 mM(b) when λ_m = 1 nm and R_m = 5 nm.

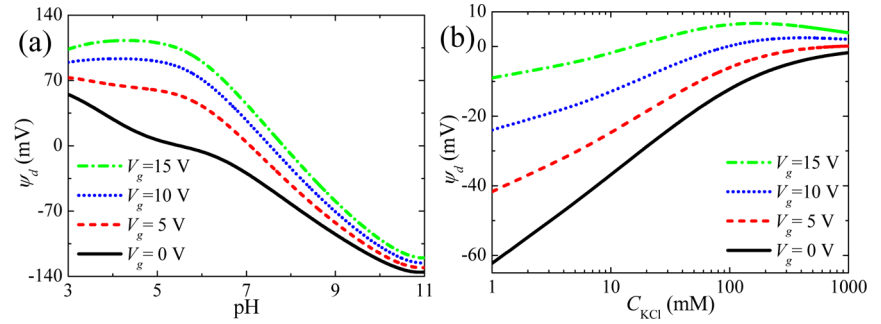

Figure 4. Variation of the Donnan potential ψ_d with the solution pH for various V_g at C_{KCl} = 1 mM, (a), and with C_{KCl} for various V_g at pH = 8, (b), when λ_m = 1 nm, and R_m = 5 nm.

unless specified elsewhere, which has been shown to be in the range for biological PE layers (i.e., 0.1−10 nm).[55,56] The remaining constants are R = 8.31 JK^{-1} mol^{-1}, T = 298 K, F = 96487 $Cmol^{-1}$, $\varepsilon_0 = 8.854 \times 10^{-12}$ $CV^{-1}m^{-1}$, ε_f = 78.5, and μ = 10^{-3} kg $m^{-1}s^{-1}$.

3.1. Code Verification. The applicability of the present numerical scheme is examined by applying it to the case of the spatial distributions of the electrical potential and the EKF velocity in a solid-state nanochannel without the PE layer. The previous results of which were solved using a rigid nanochannel by Yeh et al.[28] For comparison, we let $\lambda_m = 10^{11}$ nm and $R_m (\ll \lambda_D)$ = 0.1 nm. The former makes the present PE-modified nanochannel close to the rigid nanochannel, and the latter ensures that the thickness of the PE layer is thin enough compared to that of EDL so that the distribution of the electrical potential inside the PE layer is not appreciably influenced by its presence.[57] Since the PE layer is very thin, implying that the net charge in that layer is extremely small, the electrical potential is small in the nanochannel, as shown in Figure 2a. Figure 2 depicts the distributions of the electrical potential ϕ and the EKF velocity u near a PE-modified nanochannel. The present numerical results (symbols) agree well with the analytical results in a solid-state nanochannel (solid lines) derived by Yeh et al.[28] This suggests that the numerical scheme for the present model is correct.

In subsequent discussions, FET control of the Donnan potential and the EKF velocity in a pH-regulated PE-modified nanochannel under various key parameters, including the applied gate potential, V_g, the background solution properties such as salt concentration, C_{KCl}, and pH, and the thickness and softness of the PE layer, R_m and λ_m, respectively, are examined.

3.2. FET Control of Donnan Potential. Typically in solid-state gated nanofluidics,[15,17−19,58] the zeta potential and, accordingly, the electrokinetic transport can be regulated by controlling the gate potential, V_g, applied to the gate electrode. This comes from the fact that a strong transverse equilibrium electric field, stemming from the potential difference within the dielectric layer, makes the surface charge of the nanochannel tunable.[15,26] Figure 3 illustrates the field effect modulation of the Donnan potential, ψ_d, as a function of V_g for various levels of C_{KCl} and pH. This figure explicitly reveals that ψ_d can be modulated from negative to positive by increasing the gate potential. This field control characteristics, similar to tuning zeta potential in solid-state gated nanofluidics,[15,17−19,58] has the potential for regulating the electrokinetic transport in nanofluidics with functionalized PE brush layers. Figure 3 also shows that the critical value of V_g, $V_{g,c}$, at which ψ_d = 0, decreases with an increase in C_{KCl} (Figure 3a) and a decrease in pH if pH > 5.6 (Figure 3b). Note that if the pH < 5.6 (pH = 4 in Figure 3b), then the PE layer is positively charged and, therefore, the Donnan potential keeps positive as V_g varies. The behavior that $V_{g,c}$ decreases with an increase in C_{KCl} is due to thinner EDL at higher salt concentrations, resulting in more counterions accumulated within the PE layer and, accordingly, smaller effective charge density in the PE layer, $|\rho_m + \rho_e|$.[59] As the pH increases, more negatively charged PE∼COO^- groups are dissociated from functional groups PE∼COOH at lower proton concentration, resulting in an increase in the charge density of the PE layer ($|\rho_m|$) and $|\rho_m+\rho_e|$. Therefore, a higher $V_{g,c}$ is required as pH increases, as shown in Figure 3b.

The influences of the background salt concentration, C_{KCl}, and pH on the field effect regulation of Donnan potential, ψ_d, are depicted in Figure 4. This figure shows that if the FET is turned off (i.e., V_g = 0), then the Donnan potential can be tuned from positive to negative by the solution pH, but cannot regulated by the salt concentration. The former is expected because the considered PE layer reveals a zwitterionic, pH tunable feature, carrying positive (negative) charges if pH < 5.6

dx.doi.org/10.1021/jp504588b | J. Phys. Chem. C 2014, 118, 19806−19813

(pH > 5.6). The latter arises from the fact that the charge nature of the PE layer is not influenced by the salt concentration.[59] However, if the FET is active (i.e., $V_g > 0$), the modulated Donnan potential, as shown in Figure 4, can be regulated from negative to positive with both pH and C_{KCl}. Regulation of the Donnan potential by pH is expected since the charge property of the PE layer is pH-tunable. The latter suggests that one can even change the sign of the Donnan potential in gated PE-modified nanochannels by changing the background salt concentration. This interesting behavior is different from the FET control of the zeta potential in a solid-state nanochannel,[28−30] where the sign of the zeta potential does not change with the variation in the salt concentration.. This feature can be attributed to the ion-permeable PE layer/liquid interface, while the channel/liquid interface in a solid-state nanochannel is impermeable to ions. As C_{KCl} increases, the EDL thickness decreases, resulting in a greater number of counterions concentrated inside the PE layer. This results in a smaller magnitude of the effective charge density, $|\rho_m + \rho_e|$, of the PE layer[59] and Donnan potential, ψ_d, as observed in $V_g = 0$ V (solid line) of Figure 4b. Therefore, the Donnan potential can be regulated from negative to positive at sufficiently high salt concentration when $V_g > 0$ V. The dependence of the effective charge density within the PE layer on the salt concentration yields a salt concentration-dependent Donnan potential behavior.

Figure 4 also shows that if the gate potential is relatively high (e.g., V_g = 15 V), then ψ_d has a local maximum with the variation in pH when pH is low (Figure 4a), and as C_{KCl} varies when C_{KCl} is high (Figure 4b). Note that the charge density of the PE layer, ρ_m, is positive (negative) when pH is lower (higher) than its IEP (5.6). As described previously, an increase in C_{KCl} results in more counterions confined inside the PE layer, reducing significantly its effective charge density. However, an increase in C_{KCl} also results in an increase in $|\rho_m|$ due to the excluded effect of H^+ ions by the other counterions, K^+.[59] If the latter dominates over the former, which becomes remarkable at sufficiently high C_{KCl}, then ψ_d decreases accordingly, as depicted in the regime of high salt concentration in Figure 4b. Similarly, although a more significant deviation of pH from the IEP of the PE layer results in an increase in $|\rho_m|$, a more significant deviation of pH from 7 also increases the ionic strength (a thinner EDL thickness), lowering $|\rho_m + \rho_e|$ and, accordingly, $|\psi_d|$. Since the PE layer, if pH < 5.6 and $V_g > 0$, is positively charged, an increase in the ionic strength with decreasing pH becomes the dominant aspect of the behavior of ψ_d, and ψ_d decreases accordingly at sufficiently low pH. These V_g, pH, and salt concentration-dependent Donnan potential behaviors, therefore, imply that a FET-gated nanochannel with functionalized pH-tunable PE layers is more flexibly capable of regulating the charge property of the nanochannel and, accordingly, the transport of ions and fluid inside by adjusting the solution properties, including pH and salt concentration, and the gate potential.

Figures 3 and 4 also reveal that the FET control of ψ_d is significant when the salt concentration, C_{KCl}, is low and the pH is near the IEP of the PE layer, but becomes insignificant when C_{KCl} is high and pH appreciably deviates from the IEP. The behavior of ψ_d for various C_{KCl} is similar to the FET control of zeta potential in a solid-state nanochannel.[30] As the salt concentration increases, the EDL thickness decreases, resulting in more counterions condensed inside the PE layer. Therefore, the FET is harder to effectively tune the Donnan potential at relatively high salt concentration. Similarly, because the magnitude of the charge density of the biomimetic PE layer increases with the degree of the deviation of pH from its IEP, more counterions are condensed within the PE layer. Thus, with FET, it is harder to tune the Donnan potential when the pH significantly deviates from the IEP.

3.3. FET Control of EKF Velocity. It is known that the electrokinetic transport of fluid in a nanochannel can be controlled by FET, which has potentials in improving the performance of the nanopore sensing of DNA[51] and bionanoparticles.[52] To comprehensively understand the FET control of the EKF in a biomimetic PE-modified gated nanochannel, we plot the EKF velocity profiles near the charged nanochannel for various gate potential, V_g, background salt concentration, C_{KCl}, and pH in Figure 5. This figure shows

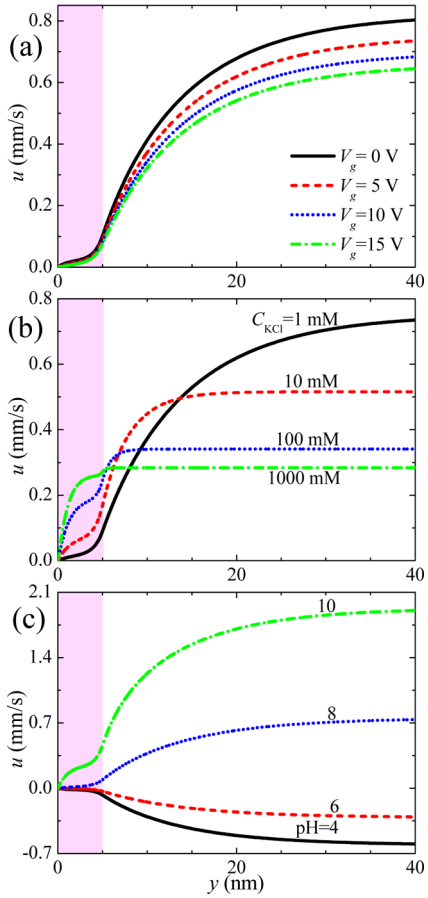

Figure 5. Spatial variations of the EKF velocity for various gate potential V_g, (a), background salt concentrations C_{KCl}, (b), and solution pH, (c), when λ_m = 1 nm, R_m = 5 nm, and E_x = 20 kV/m. (a) C_{KCl} = 1 mM and pH = 8; (b) V_g = 5 V and pH = 8; (c) V_g = 5 V and C_{KCl} = 1 mM. The pink regions highlight the region of the PE layer on the nanochannel.

that the EKF velocity profile can be regulated by controlling the values of V_g, C_{KCl}, and pH. In addition to V_g, which was verified by Benson et al.[40] for the case of the PE layer with fixed charges, the direction of the EKF can also be changed by pH, as depicted in Figure 5c. If the bulk solution pH is high (pH = 8 and 10 in Figure 5c), then the PE layer becomes negatively charged, and the resulting EKF is in the same direction of the imposed electric field. In addition, EKF velocity increases with

dx.doi.org/10.1021/jp504588b | J. Phys. Chem. C 2014, 118, 19806−19813

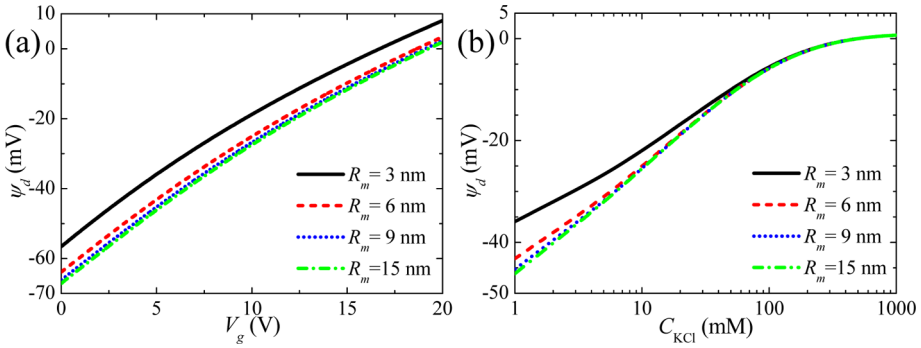

Figure 6. Variations of the Donnan potential ψ_d with the gate potential V_g, (a), and background salt concentration C_{KCl}, (b), for various thickness of the PE layer R_m at λ_m = 1 nm. (a) pH = 8 and C_{KCl} = 1 mM; (b) pH = 8 and V_g = 5 V.

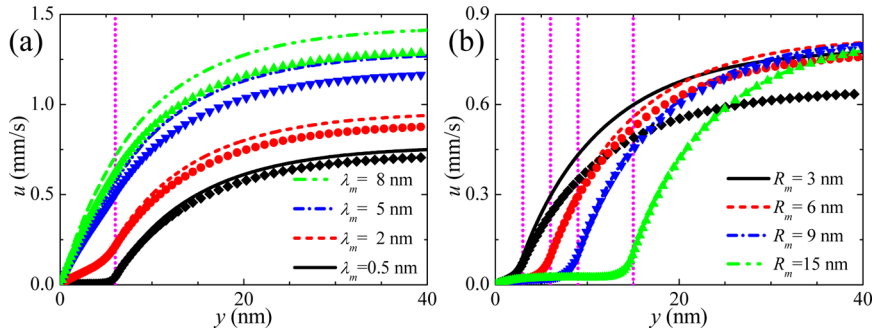

Figure 7. Spatial variations of the EKF velocity for various softness degree of the PE layer λ_m at E_x = 20 kV/m when R_m = 6 nm, pH = 8, and C_{KCl} = 1 mM, (a), and for various R_m when λ_m = 1 nm, pH = 8, and C_{KCl} = 1 mM (b). Lines and symbols denote the results at V_g = 0 and 5 V, respectively. The pink dotted lines highlight the PE layer/liquid interfaces.

increasing pH. For sufficiently low pH (pH = 4 and 6 in Figure 5c), the PE layer turns into a positively charged one. Therefore, the direction of the EKF is opposite to that of the applied electric field. This feature can be applied to control the transport of biomolecules in nanofluidics, which have a pH-tunable nature, and can be accredited to the pH regulation of the Donnan potential, as illustrated in Figures 3 and 4.

It is worth noting in Figure 5b that the EKF velocity inside the PE layer (pink region) increases with an increase in C_{KCl}, but far away from the PE layer it decreases with an increase in C_{KCl}. The latter is attributed to the decrease in Donnan potential with increasing C_{KCl}, which is accordance with the typical electroosmotic flow behavior in a solid-state nanochannel[29] where the zeta potential decreases with an increase in C_{KCl}.[29] The former is particular in PE-modified nanochannels and can be attributed to more mobile ions gathered inside the PE layer. This is because the motivity of the EKF within the PE layer is primarily dominated by the amount of mobile ions. In PE-modified nanochannels, as C_{KCl} increases, the EDL decreases accordingly, resulting in more mobile counterions gathered in the vicinity of the PE layer/liquid interface and, accordingly, a larger EKF velocity.

3.4. Influence of PE layer Properties. Because the electric potential distribution in PE-modified nanochannels is not affected by its softness parameter (λ_m),[43] we only illustrate the influence of the thickness of the PE layer, R_m, on the Donnan potential, ψ_d, in Figure 6. Figure 6a suggests that the magnitude of ψ_d modulated by the FET is insignificantly dependent on R_m. This is because an increase in R_m results in not only an increase in the net charges of the PE layer but also a decrease in the equilibrium electric field within the PE layer. The former is obstructive, but the latter is beneficial for the tuning performance of the FET. As a result, the influence of R_m on the performance of regulating Donnan potential by the FET is inappreciable. A similar phenomenon is observed in Figure 6b, where the modulated ψ_d is plotted as a function of the background salt concentration, C_{KCl}. This figure clearly shows that ψ_d is nearly independent of R_m if R_m is sufficiently large.

Figure 7 depicts the influence of the softness (λ_m) and thickness (R_m) of the PE layer on the EKF in a biomimetic PE-modified nanochannel when E_x = 20 kV/m. To make the presentation clear, we focus mainly on the EKF velocity distribution near the charged nanochannel and highlight the PE/liquid interface as a pink dotted line. Lines and symbols represent the results at V_g = 0 and 5 V, respectively. Apparently, Figure 7 shows that the EKF velocity with FET control (V_g = 5 V) is higher than that without FET control (V_g = 0 V) because the PE layer is negatively charged at pH = 8. In Figure 7a, the larger the softness parameter (the deeper the penetration depth of fluid into the PE layer) the more significant is the FET control on EKF, yielding a larger deviation of the EKF velocity between V_g = 0 and 5 V, even though the Donnan potential of PE-modified nanochannel is independent of λ_m. This can be attributed to a larger friction force stemming from the PE layer for smaller λ_m, reducing the driving force of the EKF. In addition, the difference of the EKF velocity between V_g = 0 and 5 V is remarkable if R_m is small, as shown in Figure 7b. This implies that R_m has a significant effect on the FET control of the EKF in PE-modified nanochannels for thinner PE layer. This is because the charge density of the PE layer decreases as R_m decreases, allowing the FET to tune the EKF more easily.

dx.doi.org/10.1021/jp504588b | J. Phys. Chem. C 2014, 118, 19806−19813

4. CONCLUSIONS

Controlling the Donnan potential and the electrokinetic flow (EKF) in a biomimetic polyelectrolyte (PE)-modified nanochannel, consisting of a solid-state nanochannel functionalized by a pH-regulated, zwitterionic, PE brush layer, by a field effect transistor (FET) is investigated for the first time. Taking into account practical effects such as multiple ionic species and protonation and deprotonation reactions of functional groups within the PE layer, the present study extends previous models to a case closer to reality because the charge density of the PE layer is strongly dependent on the local solution properties, including background salt concentration and pH. The obtained results show that both the Donnan potential and the EKF velocity can be regulated by the FET. Control of the Donnan potential of the PE-modified nanochannel, in turn, controls the EKF. The performance of the field effect control depends on the solution properties including the background salt concentration and pH, and the thickness and softness parameter of the PE layer. Different from the solid-state gated nanochannel, where the polarity of zeta potential can be regulated only by the transverse gate potential, the sign of the Donnan potential of the biomimetic PE-modified nanochannel can be tuned by the background salt concentration, pH, and the gate potential. The field effect on the Donnan potential depends highly on the background salt concentration and pH, but insignificantly on the thickness of the PE layer. The FET control performance of the Donnan potential is superior when the salt concentration is low and the solution pH is near the IEP of the PE layer. However, in addition to the salt concentration and pH, the softness and thickness of the PE layer significantly affect the FET control of the EKF in a PE-modified nanochannel. The degree of the FET control on the EKF is remarkable when the softness parameter of the PE layer is large and its thickness is small.

AUTHOR INFORMATION

Corresponding Authors

*Fax: +886-5-5312071; e-mail: lhyeh@yuntech.edu.tw.

*E-mail: sqian@odu.edu.

Author Contributions

[§]These authors contributed equally to this work.

Notes

The authors declare no competing financial interest.

ACKNOWLEDGMENTS

This work is supported by the Ministry of Science and Technology of the Republic of China under Grants 102-2221-E-224-052-MY3, 103-2221-E-224-039-MY3 (L.H.Y.), and 102-2622-E-224-011-CC3 (T.H.C.).

REFERENCES

(1) van der Heyden, F. H. J.; Bonthuis, D. J.; Stein, D.; Meyer, C.; Dekker, C. Electrokinetic Energy Conversion Efficiency in Nanofluidic Channels. *Nano Lett.* **2006**, *6*, 2232−2237.

(2) Yan, Y.; Sheng, Q.; Wang, C. M.; Xue, J. M.; Chang, H. C. Energy Conversion Efficiency of Nanofluidic Batteries: Hydrodynamic Slip and Access Resistance. *J. Phys. Chem. C* **2013**, *117*, 8050−8061.

(3) Siwy, Z.; Heins, E.; Harrell, C. C.; Kohli, P.; Martin, C. R. Conical-Nanotube Ion-Current Rectifiers: The Role of Surface Charge. *J. Am. Chem. Soc.* **2004**, *126*, 10850−10851.

(4) Ali, M.; Ramirez, P.; Mafe, S.; Neumann, R.; Ensinger, W. A pH-Tunable Nanofluidic Diode with a Broad Range of Rectifying Properties. *ACS Nano* **2009**, *3*, 603−608.

(5) Hou, X.; Zhang, H. C.; Jiang, L. Building Bio-Inspired Artificial Functional Nanochannels: From Symmetric to Asymmetric Modification. *Angew. Chem.-Int. Ed.* **2012**, *51*, 5296−5307.

(6) Hou, X.; Guo, W.; Jiang, L. Biomimetic Smart Nanopores and Nanochannels. *Chem. Soc. Rev.* **2011**, *40*, 2385−2401.

(7) Guo, W.; Tian, Y.; Jiang, L. Asymmetric Ion Transport through Ion-Channel-Mimetic Solid-State Nanopores. *Acc. Chem. Res.* **2013**, *46*, 2834−2846.

(8) Wu, S. M.; Wildhaber, F.; Vazquez-Mena, O.; Bertsch, A.; Brugger, J.; Renaud, P. Facile Fabrication of Nanofluidic Diode Membranes Using Anodic Aluminium Oxide. *Nanoscale* **2012**, *4*, 5718−5723.

(9) Howorka, S.; Siwy, Z. Nanopore Analytics: Sensing of Single Molecules. *Chem. Soc. Rev.* **2009**, *38*, 2360−2384.

(10) Lan, W. J.; Holden, D. A.; Zhang, B.; White, H. S. Nanoparticle Transport in Conical-Shaped Nanopores. *Anal. Chem.* **2011**, *83*, 3840−3847.

(11) Vogel, R.; Anderson, W.; Eldridge, J.; Glossop, B.; Willmott, G. A Variable Pressure Method for Characterizing Nanoparticle Surface Charge Using Pore Sensors. *Anal. Chem.* **2012**, *84*, 3125−3131.

(12) Startsev, M. A.; Inglis, D. W.; Baker, M. S.; Goldys, E. M. Nanochannel pH Gradient Electrofocusing of Proteins. *Anal. Chem.* **2013**, *85*, 7133−7138.

(13) Jeon, H.; Lee, H.; Kang, K. H.; Lim, G. Ion Concentration Polarization-Based Continuous Separation Device Using Electrical Repulsion in the Depletion Region. *Sci. Rep.* **2013**, *3*, 3483.

(14) Jiang, Z. J.; Stein, D. Charge Regulation in Nanopore Ionic Field-Effect Transistors. *Phys. Rev. E* **2011**, *83*, 031203.

(15) Karnik, R.; Fan, R.; Yue, M.; Li, D. Y.; Yang, P. D.; Majumdar, A. Electrostatic Control of Ions and Molecules in Nanofluidic Transistors. *Nano Lett.* **2005**, *5*, 943−948.

(16) Tsutsui, M.; He, Y.; Furuhashi, M.; Rahong, S.; Taniguchi, M.; Kawai, T. Transverse Electric Field Dragging of DNA in a Nanochannel. *Sci. Rep.* **2012**, *2*, 394.

(17) Paik, K. H.; Liu, Y.; Tabard-Cossa, V.; Waugh, M. J.; Huber, D. E.; Provine, J.; Howe, R. T.; Dutton, R. W.; Davis, R. W. Control of DNA Capture by Nanofluidic Transistors. *ACS Nano* **2012**, *6*, 6767−6775.

(18) Guan, W. H.; Fan, R.; Reed, M. A. Field-Effect Reconfigurable Nanofluidic Ionic Diodes. *Nat. Commun.* **2011**, *2*, 506.

(19) Guan, W. J.; Reed, M. A. Electric Field Modulation of the Membrane Potential in Solid-State Ion Channels. *Nano Lett.* **2012**, *12*, 6441−6447.

(20) Daiguji, H.; Yang, P. D.; Majumdar, A. Ion Transport in Nanofluidic Channels. *Nano Lett.* **2004**, *4*, 137−142.

(21) Daiguji, H.; Oka, Y.; Shirono, K. Nanofluidic Diode and Bipolar Transistor. *Nano Lett.* **2005**, *5*, 2274−2280.

(22) Singh, K. P.; Kumar, M. Effect of Gate Length and Dielectric Thickness on Ion and Fluid Transport in a Fluidic Nanochannel. *Lab Chip* **2012**, *12*, 1332−1339.

(23) Jin, X. Z.; Aluru, N. R. Gated Transport in Nanofluidic Devices. *Microfluid. Nanofluid.* **2011**, *11*, 297−306.

(24) Pardon, G.; van der Wijngaart, W. Modeling and Simulation of Electrostatically Gated Nanochannels. *Adv. Colloid Interface Sci.* **2013**, *199*, 78−94.

(25) He, Y. H.; Tsutsui, M.; Fan, C.; Taniguchi, M.; Kawai, T. Gate Manipulation of DNA Capture into Nanopores. *ACS Nano* **2011**, *5*, 8391−8397.

(26) Ai, Y.; Liu, J.; Zhang, B. K.; Qian, S. Field Effect Regulation of DNA Translocation through a Nanopore. *Anal. Chem.* **2010**, *82*, 8217−8225.

(27) He, Y. H.; Tsutsui, M.; Fan, C.; Taniguchi, M.; Kawai, T. Controlling DNA Translocation through Gate Modulation of Nanopore Wall Surface Charges. *ACS Nano* **2011**, *5*, 5509−5518.

(28) Yeh, L. H.; Xue, S.; Joo, S. W.; Qian, S.; Hsu, J. P. Field Effect Control of Surface Charge Property and Electroosmotic Flow in Nanofluidics. *J. Phys. Chem. C* **2012**, *116*, 4209−4216.

(29) Hughes, C.; Yeh, L. H.; Qian, S. Field Effect Modulation of Surface Charge Property and Electroosmotic Flow in a Nanochannel: Stern Layer Effect. *J. Phys. Chem. C* **2013**, *117*, 9322−9331.
(30) Xue, S.; Yeh, L. H.; Ma, Y.; Qian, S. Tunable Streaming Current in a pH-Regulated Nanochannel by a Field Effect Transistor. *J. Phys. Chem. C* **2014**, *118*, 6090−6099.
(31) Yameen, B.; Ali, M.; Neumann, R.; Ensinger, W.; Knoll, W.; Azzaroni, O. Single Conical Nanopores Displaying pH-Tunable Rectifying Characteristics. Manipulating Ionic Transport With Zwitterionic Polymer Brushes. *J. Am. Chem. Soc.* **2009**, *131*, 2070−2071.
(32) Hou, X.; Yang, F.; Li, L.; Song, Y. L.; Jiang, L.; Zhu, D. B. A Biomimetic Asymmetric Responsive Single Nanochannel. *J. Am. Chem. Soc.* **2010**, *132*, 11736−11742.
(33) Zhang, L. X.; Cai, S. L.; Zheng, Y. B.; Cao, X. H.; Li, Y. Q. Smart Homopolymer Modification to Single Glass Conical Nanopore Channels: Dual-Stimuli-Actuated Highly Efficient Ion Gating. *Adv. Funct. Mater.* **2011**, *21*, 2103−2107.
(34) Zhang, H. C.; Hou, X.; Zeng, L.; Yang, F.; Li, L.; Yan, D. D.; Tian, Y.; Jiang, L. Bioinspired Artificial Single Ion Pump. *J. Am. Chem. Soc.* **2013**, *135*, 16102−16110.
(35) Kowalczyk, S. W.; Kapinos, L.; Blosser, T. R.; Magalhaes, T.; van Nies, P.; Lim, R. Y. H.; Dekker, C. Single-Molecule Transport Across an Individual Biomimetic Nuclear Pore Complex. *Nat. Nanotechnol.* **2011**, *6*, 433−438.
(36) Liu, J.; Pham, P.; Haguet, V.; Sauter-Starace, F.; Leroy, L.; Roget, A.; Descamps, E.; Bouchet, A.; Buhot, A.; Mailey, P.; Livache, T. Polarization-Induced Local Pore-Wall Functionalization for Biosensing: From Micropore to Nanopore. *Anal. Chem.* **2012**, *84*, 3254−3261.
(37) Liu, N. N.; Jiang, Y. N.; Zhou, Y. H.; Xia, F.; Guo, W.; Jiang, L. Two-Way Nanopore Sensing of Sequence-Specific Oligonucleotides and Small-Molecule Targets in Complex Matrices Using Integrated DNA Supersandwich Structures. *Angew. Chem.—Int. Ed.* **2013**, *52*, 2007−2011.
(38) Ohshima, H.; Ohki, S. Donnan Potential and Surface-Potential of a Charged Membrane. *Biophys. J.* **1985**, *47*, 673−678.
(39) Barbati, A. C.; Kirby, B. J. Soft Diffuse Interfaces in Electrokinetics—Theory and Experiment for Transport in Charged Diffuse Layers. *Soft Matter* **2012**, *8*, 10598−10613.
(40) Benson, L.; Yeh, L. H.; Chou, T. H.; Qian, S. Z. Field Effect Regulation of Donnan Potential and Electrokinetic Flow in a Functionalized Soft Nanochannel. *Soft Matter* **2013**, *9*, 9767−9773.
(41) Peleg, O.; Tagliazucchi, M.; Kroger, M.; Rabin, Y.; Szleifer, I. Morphology Control of Hairy Nanopores. *ACS Nano* **2011**, *5*, 4737−4747.
(42) Duval, J. F. L.; Ohshima, H. Electrophoresis of Diffuse Soft Particles. *Langmuir* **2006**, *22*, 3533−3546.
(43) Yeh, L. H.; Zhang, M.; Hu, N.; Joo, S. W.; Qian, S.; Hsu, J. P. Electrokinetic Ion and Fluid Transport in Nanopores Functionalized by Polyelectrolyte Brushes. *Nanoscale* **2012**, *4*, 5169−5177.
(44) van der Heyden, F. H. J.; Bonthuis, D. J.; Stein, D.; Meyer, C.; Dekker, C. Power Generation by Pressure-Driven Transport of Ions in Nanofluidic Channels. *Nano Lett.* **2007**, *7*, 1022−1025.
(45) Louer, A. C.; Plecis, A.; Pallandre, A.; Galas, J. C.; Estevez-Torres, A.; Haghiri-Gosnet, A. M. Pressure-Assisted Selective Preconcentration in a Straight Nanochannel. *Anal. Chem.* **2013**, *85*, 7948−7956.
(46) Schoch, R. B.; Han, J. Y.; Renaud, P. Transport Phenomena in Nanofluidics. *Rev. Mod. Phys.* **2008**, *80*, 839−883.
(47) Yeh, L. H.; Zhang, M.; Qian, S.; Hsu, J. P.; Tseng, S. Ion Concentration Polarization in Polyelectrolyte-Modified Nanopores. *J. Phys. Chem. C* **2012**, *116*, 8672−8677.
(48) Liu, K. L.; Hsu, J. P.; Tseng, S. Capillary Osmosis in a Charged Nanopore Connecting Two Large Reservoirs. *Langmuir* **2013**, *29*, 9598−9603.
(49) Yeh, L. H.; Hsu, J. P.; Qian, S.; Tseng, S. J. Counterion Condensation in pH-Regulated Polyelectrolytes. *Electrochem. Commun.* **2012**, *19*, 97−100.
(50) Yeh, L. H.; Zhang, M.; Qian, S. Ion Transport in a pH-Regulated Nanopore. *Anal. Chem.* **2013**, *85*, 7527−7534.
(51) Yeh, L. H.; Zhang, M.; Qian, S.; Hsu, J. P. Regulating DNA Translocation through Functionalized Soft Nanopores. *Nanoscale* **2012**, *4*, 2685−2693.
(52) Yeh, L. H.; Zhang, M. K.; Joo, S. W.; Qian, S.; Hsu, J. P. Controlling pH-Regulated Bionanoparticles Translocation through Nanopores with Polyelectrolyte Brushes. *Anal. Chem.* **2012**, *84*, 9615−9622.
(53) Zeng, Z. P.; Ai, Y.; Qian, S. Z. pH-Regulated Ionic Current Rectification in Conical Nanopores Functionalized with Polyelectrolyte brushes. *Phys. Chem. Chem. Phys.* **2014**, *16*, 2465−2474.
(54) Switzer, R.; Garrity, L. *Experimental Biochemistry*; W. H. Freeman Publishing: New York, 1999.
(55) Duval, J. F. L.; Gaboriaud, F. Progress in Electrohydrodynamics of Soft Microbial Particle Interphases. *Curr. Opin. Colloid Interface Sci.* **2010**, *15*, 184−195.
(56) Zimmermann, R.; Dukhin, S. S.; Werner, C.; Duval, J. F. L. On the Use of Electrokinetics for Unraveling Charging and Structure of Soft Planar Polymer Films. *Curr. Opin. Colloid Interface Sci.* **2013**, *18*, 83−92.
(57) Yeh, L. H.; Hsu, J. P.; Tseng, S. Electrophoresis of a Membrane-Coated Cylindrical Particle Positioned Eccentrically along the Axis of a Narrow Cylindrical Pore. *J. Phys. Chem. C* **2010**, *114*, 16576−16587.
(58) Karnik, R.; Castelino, K.; Majumdar, A. Field-Effect Control of Protein Transport in a Nanofluidic Transistor Circuit. *Appl. Phys. Lett.* **2006**, *88*, 123114.
(59) Yeh, L. H.; Tai, Y. H.; Wang, N.; Hsu, J. P.; Qian, S. Electrokinetics of pH-Regulated Zwitterionic Polyelectrolyte Nanoparticles. *Nanoscale* **2012**, *4*, 7575−7584.